

A dynamic finite element method for the estimation of cable tension

Yonghui Huang^{1a}, Quan Gan^{2b}, Shiping Huang^{*3} and Ronghui Wang^{3c}

¹Guangzhou University-Tamkang University Joint Research Center for Engineering Structure Disaster Prevention and Control, Guangzhou University, Guangzhou 510006, China

²Network & Educational Technology Center, Jinan University, Guangzhou 510632, China

³School of Civil Engineering and Transportation, South China University of Technology, Guangzhou 510640, China

(Received March 26, 2018, Revised September 11, 2018, Accepted September 12, 2018)

Abstract. Cable supported structures have been widely used in civil engineering. Cable tension estimation has great importance in cable supported structures' analysis, ranging from design to construction and from inspection to maintenance. Even though the Bernoulli-Euler beam element is commonly used in the traditional finite element method for calculation of frequency and cable tension estimation, many elements must be meshed to achieve accurate results, leading to expensive computation. To improve the accuracy and efficiency, a dynamic finite element method for estimation of cable tension is proposed. In this method, following the dynamic stiffness matrix method, frequency-dependent shape functions are adopted to derive the stiffness and mass matrices of an exact beam element that can be used for natural frequency calculation and cable tension estimation. An iterative algorithm is used for the exact beam element to determine both the exact natural frequencies and the cable tension. Illustrative examples show that, compared with the cable tension estimation method using the conventional beam element, the proposed method has a distinct advantage regarding the accuracy and the computational time.

Keywords: dynamic finite element; frequency-dependent shape function; frequency calculation; cable tension estimation

1. Introduction

Cable supported structures have been widely used in civil engineering. The dynamic response of the cable, such as the cable frequency and tension, has great importance in cable supported structures' analysis (Ma 2017, Maes *et al.* 2017, Park and Kim 2014), ranging from design to construction and from inspection to maintenance. To date, the finite element method is widely used in the dynamics response of the structures. However, the accuracy of the numerical results depends not only the fitness of the physical model to the true structure but also the use of the proper element. For the conventional static finite element method in which formulations are based on fixed shape functions, the common method to improve the precision is to increase the quantity of discrete elements (Zienkiewicz and Taylor 2000). This approach would result in good accuracy for static analysis when the number of degrees of freedom (DOFs) is adequate. However, for structural dynamic analysis, the shape function of the element is not a fixed one for different modes because the modal shapes are

frequency-dependent (Leung 1992, Banerjee 1997, Hashemi and Richard 1994, Yuan *et al.* 2007, Ma 2010). In that case, even though the number of DOFs is sufficient, the calculated results are not exact, especially for the higher-order frequency responses and complex structures (Yucel *et al.* 2014). To prove the accuracy of dynamic analysis, a new method named dynamic stiffness matrix (DSM) method was proposed by Kolousek in 1941 (Kolousek 1941). In the DSM method, the shape functions of the element are derived from the closed-form analytical solution of the differential equation of the element, hence the stiffness and mass matrices of the element are justifiably called 'exact'.

The DSM method was firstly proposed by Kolousek (Kolousek 1941), who later introduced the method into a text book (Kolousek 1973) for the case of a Bernoulli-Euler beam. Later, in order to consider the effect of axial load, Mohsin and Sadek (1968) developed the dynamic stiffness matrix of an axially loaded beam but ignored the shear effect. Then, Cheng (1970) and Wang *et al.* (1970) developed the dynamic stiffness formulation for a Timoshenko beam based on considering the effect of shear deformation and rotatory inertia, but in this formulation, the effect of axial force is not considered. Subsequently, Howson and Williams (1973), Cheng and Tseng (1973) developed the dynamic stiffness matrix of an axially loaded Timoshenko beam. The key component used in the DSM method is the dynamic stiffness matrix accounting for both stiffness and mass properties which are frequency dependent. By solving the nonlinear eigenvalue problems, infinite frequencies and mode shapes of the structures can be obtained theoretically from the DSM. In the early stage, solving such nonlinear eigenvalue problems is very difficult

*Corresponding author, Associate Professor

E-mail: ctasihuang@scut.edu.cn

^aAssociate Professor

E-mail: huangyh@gzhu.edu.cn

^bSenior experimentalist

E-mail: gq@jnu.edu.cn

^cProfessor

E-mail: rhwang2002@163.com

and thus limits the application of the DSM method. Subsequently, Wittrick and Williams (1971) developed a reliable and efficient algorithm to solve such problems, generally known as the W–W algorithm in the literature. Afterwards, the DSM method has been developed rapidly and expanded to many other structures for nonlinear analysis (Lunden and Akesson 1983, Banerjee and Williams 1985, Williams and Kennedy 1987, Issa 1988, Hallauer and Liu 1982, Friberg 1983, Banerjee 1989, Banerjee and Williams 1992, Banerjee and Fisher 1992).

The aforementioned research studies are mainly focused on the calculation of the dynamic characterizes, i.e., frequencies and modal shapes. The DSM method and the W–W algorithm are appropriate for use in frequency calculation. Furthermore, there also exists another inverse problem, i.e., axial load estimation, which is even more important for the structural design, construction, inspection and maintenance (Wang *et al.* 2015, Bao *et al.* 2017, Huang *et al.* 2017, Kim 2018, Mohammadnejad 2018). Some of the aforementioned literature considered the effect of axial load on the frequencies of the beam. However, there are rare studies on the inverse problem, i.e., identifying the axial load from the measured frequencies for problems that are not appropriate for the DSM method and W–W algorithm.

Cable tension estimation is very important for cable supported structures. There are two primary types of cable tension estimation methods: the explicit formulae method and the finite element method (Huang *et al.* 2014, 2015). The explicit formulae method can only be used for cables with simple boundary conditions, in which the relationship between the measured frequency and cable tension can be expressed in closed form (Yan *et al.* 2015). For the situations in which the explicit formulae method cannot work, the finite element method is used as an alternative. Kim and Park (2007) proposed a technique to estimate the cable tension from the measured natural frequencies by using finite element analysis for system identification. Wang *et al.* (2011) proposed a finite element method to calculate the tension in cables with intermediate supports. Liao *et al.* (2012) proposed a multiple frequency method for cable tension estimation and structural parameter identification based on a finite element model accounting for cable bending stiffness, sag-extensibility, and other geometric and material parameters. However, all of those studies used the conventional finite element method. For the aforementioned reasons, the conventional finite element method is not accurate and efficient enough.

In this study, we propose an intermediate approach called the dynamic finite element method, in which the conventional finite element method is combined with the DSM method to estimate the cable frequency and tension accurately and efficiently. This combination is achieved through the following steps: first, the exact analytical solution of the differential equation of axially load beam, which is nonlinear and frequency-dependent, is used as the shape functions of the element; next, the stiffness and mass matrices of the element are derived by using the variation principle of potential energy; subsequently, the cables are divided into several proposed exact elements, and the global

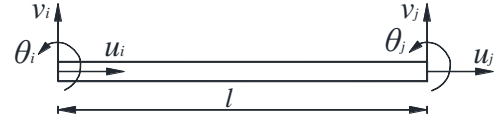


Fig. 1 Nodal displacements of the element

stiffness and mass matrices are assembled; afterwards, the iterative algorithm and finite element program are developed to implement the exact beam element to determine both the exact natural frequencies and cable tension; last, illustrative examples are conducted to verify the correctness of the proposed new element and method.

2. Shape function of the element

If the sag of the cable is negligible, then the tensioned cable can be simulated using the axially loaded Euler-beam element (Wang *et al.* 2011); the nodal displacements of the new element are shown in Fig. 1.

The general solution of the transverse vibration of the axially loaded Euler-beam is (Zienkiewicz and Taylor 2000)

$$v(x) = a_1 \sin(\delta x) + a_2 \cos(\delta x) + a_3 \sinh(\varepsilon x) + a_4 \cosh(\varepsilon x) \quad (1)$$

where

$$\delta = \sqrt{\sqrt{\zeta^4 + \gamma^4} - \zeta^2} \quad (2a)$$

$$\varepsilon = \sqrt{\sqrt{\zeta^4 + \gamma^4} + \zeta^2} \quad (2b)$$

$$\gamma^4 = \frac{m\omega^2}{EI} \quad (2c)$$

$$\zeta^2 = \frac{T}{2EI} \quad (2d)$$

The general solution of the axial vibration is (Ma 2008)

$$u(x) = b_1 \cos(\alpha x) + b_2 \sin(\alpha x) \quad (3)$$

Where

$$\alpha = \frac{m\omega^2}{EA} \quad (4)$$

Eqs. (1) and (4) can also be expressed as the following matrix multiplication form

$$v(x) = \begin{bmatrix} \sin(\delta x) & \cos(\delta x) & \sinh(\varepsilon x) & \cosh(\varepsilon x) \end{bmatrix} \times [a_1 \ a_2 \ a_3 \ a_4]^T = \mathbf{H}_1 \mathbf{a} \quad (5)$$

$$u(x) = \begin{bmatrix} \cos(\alpha x) & \sin(\alpha x) \end{bmatrix} [b_1 \ b_2]^T = \mathbf{H}_2 \mathbf{b} \quad (6)$$

Where \mathbf{a} and \mathbf{b} are vectors of undetermined coefficients of displacement mode and can be expressed by nodal

displacement. The vectors of axial displacement, transverse displacement and angle of deflection of nodes can be expressed as

$$\delta_v = [v_i \ \theta_i \ v_j \ \theta_j]^T \quad (7a)$$

$$\delta_u = [u_i \ u_j]^T \quad (7b)$$

Combining Eqs. (5) and (7a) yields

$$\delta_v = \begin{bmatrix} 0 & 1 & 0 & 1 \\ \delta & 0 & \varepsilon & 0 \\ \sin(\delta l) & \cos(\delta l) & sh(\varepsilon l) & ch(\varepsilon l) \\ \delta \cos(\delta l) & -\delta \sin(\delta l) & \varepsilon ch(\varepsilon l) & \varepsilon sh(\varepsilon l) \end{bmatrix} \begin{bmatrix} a_1 \\ a_2 \\ a_3 \\ a_4 \end{bmatrix} = \mathbf{A}_v \mathbf{a} \quad (8)$$

Combining Eqs. (6) and (7b) yields

$$\delta_u = \begin{bmatrix} 1 & 0 \\ \cos(\alpha l) & \sin(\alpha l) \end{bmatrix} \begin{bmatrix} b_1 \\ b_2 \end{bmatrix} = \mathbf{A}_u \mathbf{b} \quad (9)$$

Thus, the matrices of the undetermined coefficients of displacement mode can be given as

$$\mathbf{a} = \mathbf{A}_v^{-1} \delta_v = \mathbf{C}_v \delta_v \quad (10a)$$

$$\mathbf{b} = \mathbf{A}_u^{-1} \delta_u = \mathbf{C}_u \delta_u \quad (10b)$$

Where \mathbf{C}_v and \mathbf{C}_u are the inverse matrices of \mathbf{A}_v and \mathbf{A}_u , respectively; they are

$$\mathbf{C}_v = \frac{1}{a} \begin{bmatrix} -\frac{\varepsilon}{\delta} \cdot c \cdot sh - s \cdot ch & \frac{1-c \cdot ch}{\delta} - \frac{s \cdot sh}{\varepsilon} & \frac{\varepsilon}{\delta} \cdot sh + s & \frac{c-ch}{\delta} \\ \frac{\varepsilon}{\delta} \cdot s \cdot sh - c \cdot ch + 1 & \frac{s \cdot ch}{\delta} - \frac{c \cdot sh}{\varepsilon} & -ch + c & -\frac{s}{\delta} + \frac{sh}{\varepsilon} \\ c \cdot sh + \frac{\delta}{\varepsilon} \cdot s \cdot ch & \frac{s \cdot sh}{\delta} + \frac{1-c \cdot ch}{\varepsilon} & -sh - \frac{\delta}{\varepsilon} \cdot s & \frac{ch-c}{\varepsilon} \\ -c \cdot ch - \frac{\delta}{\varepsilon} \cdot s \cdot sh + 1 & -\frac{s \cdot ch}{\delta} + \frac{c \cdot sh}{\varepsilon} & ch - c & \frac{s}{\delta} - \frac{sh}{\varepsilon} \end{bmatrix} \quad (11)$$

$$\mathbf{C}_u = \begin{bmatrix} 1 & 0 \\ -\cot(\alpha l) & \csc(\alpha l) \end{bmatrix} \quad (12)$$

In Eq. (11)

$$s = \sin(\delta l), c = \cos(\delta l), sh = \sinh(\varepsilon l), ch = \cosh(\varepsilon l)$$

$$a = \left(\frac{\varepsilon}{\delta} - \frac{\delta}{\varepsilon} \right) \cdot \sin(\delta l) \cdot \sinh(\varepsilon l) + 2(1 - \cos(\delta l)) \cdot \cosh(\varepsilon l) \quad (13)$$

Substituting Eq. (10a) into Eqs. (5) and Eq. (10b) into Eq. (6), the continuous displacement of the element can be expressed as a function of the nodal displacement as follows

$$v(x) = \mathbf{N}_v \delta_v \quad (14a)$$

$$u(x) = \mathbf{N}_u \delta_u \quad (14b)$$

where

$$\mathbf{N}_v = \mathbf{H}_1 \mathbf{C}_v = [N_{v1} \ N_{v2} \ N_{v3} \ N_{v4}] \quad (15a)$$

$$\mathbf{N}_u = \mathbf{H}_2 \mathbf{C}_u = [N_{u1} \ N_{u2}] \quad (15b)$$

and

$$\begin{aligned} N_{v1} &= \frac{\sin(\delta x)}{M} [-\varepsilon sh(\varepsilon c + \delta s)] + \cos(\delta x) [\varepsilon sh(\varepsilon s - \delta c)] + \\ &\quad \sinh(\varepsilon x) [\delta sh(\varepsilon c + \delta s)] + \cosh(\varepsilon x) [\delta(\varepsilon - (\varepsilon c + \delta s)ch)] \\ N_{v2} &= \frac{\sin(\delta x)}{M} [-ch(\varepsilon c + \delta s)] + \cos(\delta x) [ch(\varepsilon s - \delta c)] + \\ &\quad \sinh(\varepsilon x) [sh(\varepsilon s - \delta c) + \delta] + \cosh(\varepsilon x) [ch(\delta c - \varepsilon s)] \\ N_{v3} &= \frac{\sin(\delta x)}{M} [\varepsilon(\varepsilon sh + \delta s)] + \cos(\delta x) [\delta \varepsilon(c - ch)] - \\ &\quad \sinh(\varepsilon x) [\delta(\varepsilon sh + \delta s)] + \cosh(\varepsilon x) [\delta \varepsilon(ch - c)] \\ N_{v4} &= \frac{\sin(\delta x)}{M} [\varepsilon(c - sh)] + \cos(\delta x) [\delta ch - \varepsilon s] + \\ &\quad \sinh(\varepsilon x) [\delta(sh - c)] + \cosh(\varepsilon x) [(\varepsilon s - \delta ch)] \\ M &= \varepsilon \delta [1 - c(ch + sh)] + s[\varepsilon^2 sh - \delta^2 ch] \\ N_{u1} &= \cos(\alpha x) - \cot(\alpha l) \sin(\alpha x) \\ N_{u2} &= \csc(\alpha l) \sin(\alpha x) \end{aligned}$$

3. Stiffness and mass matrices of the element

3.1 Axial stiffness matrix

The strain energy induced by axial deformation is

$$\Pi_u = \frac{1}{2} \int_0^l EA \varepsilon^2 dx = \frac{EA}{2} \int_0^l (u')^2 dx \quad (16)$$

where E , A are the Young's modulus and the sectional area of the element, respectively.

The variation of the axial strain energy is

$$\begin{aligned} \delta \Pi_u &= EA \int_0^l \delta u'(u') dx \\ &= EA \delta \delta_u^T \int_0^l \mathbf{N}_u'^T \mathbf{N}_u' dx \delta_u \end{aligned} \quad (17)$$

Using the standard procedure of the finite element method, the axial stiffness matrix of the element can be expressed as

$$\mathbf{K}_u(\omega) = EA \int_0^l \mathbf{N}_u'^T \mathbf{N}_u' dx \quad (18)$$

Substituting Eq. (15b) into Eq. (18) and integrating yields

$$\begin{aligned} \mathbf{K}_u(\omega) &= \frac{EA}{l} \frac{\alpha l}{2 \sin(\alpha l)} \\ &\quad \times \begin{bmatrix} \cos(\alpha l) + \alpha l \csc(\alpha l) & -(1 + \alpha l \cot(\alpha l)) \\ -(1 + \alpha l \cot(\alpha l)) & \cos(\alpha l) + \alpha l \csc(\alpha l) \end{bmatrix} \quad (19) \end{aligned}$$

3.2 Bending stiffness matrix

The bending strain energy induced by bending

deformation is

$$\Pi_v = \int_0^l \frac{EI}{2} (v'')^2 dx \quad (20)$$

where E , I are the Young's modulus and cross sectional moment of inertia of the element, respectively.

The variation of the bending strain energy is

$$\delta \Pi_v = \frac{EI}{2} \int_0^l 2(v'') \cdot \delta v'' \cdot dx = EI \int_0^l v'' \cdot \delta v'' dx \quad (21)$$

Substituting Eq. (14a) into Eq. (21) yields

$$\delta \Pi_v = \delta \mathbf{\delta}_v^T \left(EI \int_0^l \mathbf{N}_v''^T \mathbf{N}_v'' dx \right) \mathbf{\delta}_v \quad (22)$$

Using the standard procedure of the finite element method, the bending stiffness matrix of the element can be expressed as

$$\mathbf{K}_v(\omega) = EI \int_0^l \mathbf{N}_v''^T \mathbf{N}_v'' dx \quad (23)$$

From Eq. (15a), one obtains

$$\mathbf{N}_v'' = \mathbf{H}_1'' \mathbf{C}_v \quad (24)$$

Thus

$$\begin{aligned} \mathbf{K}_v(\omega) &= EI \int_0^l \left(\mathbf{H}_1'' \mathbf{C}_v \right)^T \left(\mathbf{H}_1'' \mathbf{C}_v \right) dx \\ &= EI \mathbf{C}_v^T \int_0^l \mathbf{H}_1''^T \mathbf{H}_1'' dx \mathbf{C}_v = EI \mathbf{C}_v^T \mathbf{B} \mathbf{C}_v \end{aligned} \quad (25)$$

where

$$\mathbf{H}_1'' = \begin{bmatrix} -\delta^2 \sin(\delta x) & -\delta^2 \cos(\delta x) & \varepsilon^2 \sinh(\varepsilon x) & \varepsilon^2 \cosh(\varepsilon x) \end{bmatrix} \quad (26)$$

and

$$\begin{aligned} \mathbf{B} &= \int_0^l \mathbf{H}_1''^T \mathbf{H}_1'' dx \\ &= \delta^2 \varepsilon^2 \begin{bmatrix} \frac{\delta^2}{\varepsilon^2} S_{11} & \frac{\delta^2}{\varepsilon^2} S_{12} & -S_{13} & -S_{14} \\ & \frac{\delta^2}{\varepsilon^2} S_{22} & -S_{23} & -S_{24} \\ & & \frac{\varepsilon^2}{\delta^2} S_{33} & \frac{\varepsilon^2}{\delta^2} S_{34} \\ \text{symmetry} & & & \frac{\varepsilon^2}{\delta^2} S_{44} \end{bmatrix} \end{aligned} \quad (27)$$

where

$$\begin{aligned} \mathbf{S} &= \begin{bmatrix} S_{11} & S_{12} & S_{13} & S_{14} \\ & S_{22} & S_{23} & S_{24} \\ & & S_{33} & S_{34} \\ \text{symmetry} & & & S_{44} \end{bmatrix} \\ &= \begin{bmatrix} \frac{\delta l - s \cdot c}{2\delta} & \frac{s^2}{2\delta} & \frac{\varepsilon \cdot s \cdot ch - \delta \cdot c \cdot sh}{\delta^2 + \varepsilon^2} & \frac{\varepsilon \cdot s \cdot sh - \delta \cdot c \cdot ch + \delta}{\delta^2 + \varepsilon^2} \\ \frac{\delta l + s \cdot c}{2\delta} & \frac{\varepsilon \cdot c \cdot ch + \delta \cdot s \cdot sh - \varepsilon}{\delta^2 + \varepsilon^2} & \frac{\varepsilon \cdot c \cdot sh + \delta \cdot s \cdot ch}{\delta^2 + \varepsilon^2} & \frac{\varepsilon \cdot c \cdot sh + \delta \cdot s \cdot ch}{\delta^2 + \varepsilon^2} \\ & \frac{-\varepsilon l + sh \cdot ch}{2\varepsilon} & \frac{sh^2}{2\varepsilon} & \frac{sh \cdot ch}{2\varepsilon} \\ \text{symmetry} & & & \frac{\varepsilon l + sh \cdot ch}{2\varepsilon} \end{bmatrix} \end{aligned} \quad (28)$$

Substituting Eq. (11) and Eq. (27) into Eq. (25), one obtains the bending stiffness matrix as follows

$$\mathbf{K}_v(\omega) = \begin{bmatrix} K_{v11} & K_{v12} & K_{v13} & K_{v14} \\ K_{v21} & K_{v22} & K_{v23} & K_{v24} \\ K_{v31} & K_{v32} & K_{v33} & K_{v34} \\ K_{v41} & K_{v42} & K_{v43} & K_{v44} \end{bmatrix} \quad (29)$$

The detailed expression of K_{vij} is very complex and can be obtained from symbolic computation using mathematical software, such as Maple, from Eq. (25).

3.3 Stiffness matrix of the axial force

The axial strain energy induced by the axial force is (Wang *et al.* 2011)

$$\Pi_t = \frac{T}{2} \int_0^l (v')^2 dx \quad (30)$$

The variation of the strain energy is

$$\delta \Pi_t = \frac{T}{2} \int_0^l 2v' \cdot \delta v' \cdot dx = T \int_0^l v' \cdot \delta v' dx \quad (31)$$

From Eq. (14a), one obtains

$$\delta \Pi_t = \delta \mathbf{\delta}_v^T \left(T \int_0^l \mathbf{N}_v'^T \mathbf{N}_v' dx \right) \mathbf{\delta}_v = \delta \mathbf{\delta}_v^T \mathbf{K}_t \mathbf{\delta}_v \quad (32)$$

From Eq. (15a), one obtains

$$\mathbf{N}_v' = \mathbf{H}_1' \mathbf{C}_v \quad (33)$$

Thus,

$$\begin{aligned} \mathbf{K}_t(\omega) &= T \int_0^l \left(\mathbf{H}_1' \mathbf{C}_v \right)^T \left(\mathbf{H}_1' \mathbf{C}_v \right) dx \\ &= T \mathbf{C}_v^T \int_0^l \mathbf{H}_1'^T \mathbf{H}_1' dx \mathbf{C}_v = T \mathbf{C}_v^T \mathbf{L} \mathbf{C}_v \end{aligned} \quad (34)$$

where

$$\mathbf{H}_1' = \begin{bmatrix} \delta \cos(\delta x) & -\delta \sin(\delta x) & \varepsilon \cosh(\varepsilon x) & \varepsilon \sinh(\varepsilon x) \end{bmatrix} \quad (35)$$

and

$$\begin{aligned} \mathbf{L} &= \int_0^l \mathbf{H}_1'^T \mathbf{H}_1' dx \\ &= \delta^2 \varepsilon^2 \begin{bmatrix} \frac{\delta^2}{\varepsilon^2} S_{11} & \frac{\delta^2}{\varepsilon^2} S_{12} & -S_{13} & -S_{14} \\ & \frac{\delta^2}{\varepsilon^2} S_{22} & -S_{23} & -S_{24} \\ & & \frac{\varepsilon^2}{\delta^2} S_{33} & \frac{\varepsilon^2}{\delta^2} S_{34} \\ \text{symmetry} & & & \frac{\varepsilon^2}{\delta^2} S_{44} \end{bmatrix} \end{aligned} \quad (36)$$

where

$$\mathbf{S} = \begin{bmatrix} S_{11} & S_{12} & S_{13} & S_{14} \\ & S_{22} & S_{23} & S_{24} \\ & & S_{33} & S_{34} \\ \text{symmetry} & & & S_{44} \end{bmatrix} = \begin{bmatrix} \frac{\delta l - s \cdot c}{2\delta} & \frac{s^2}{2\delta} & \frac{\varepsilon \cdot s \cdot ch - \delta \cdot c \cdot sh}{\delta^2 + \varepsilon^2} & \frac{\varepsilon \cdot s \cdot sh - \delta \cdot c \cdot ch + \delta}{\delta^2 + \varepsilon^2} \\ & \frac{\delta l + s \cdot c}{2\delta} & \frac{\varepsilon \cdot c \cdot ch + \delta \cdot s \cdot sh - \varepsilon}{\delta^2 + \varepsilon^2} & \frac{\varepsilon \cdot c \cdot sh + \delta \cdot s \cdot ch}{\delta^2 + \varepsilon^2} \\ & & \frac{-\varepsilon l + sh \cdot ch}{2\varepsilon} & \frac{sh^2}{2\varepsilon} \\ \text{symmetry} & & & \frac{\varepsilon l + sh \cdot ch}{2\varepsilon} \end{bmatrix} \quad (37)$$

Substituting Eqs. (11) and (36) into Eq. (34), the stiffness matrix corresponding to the initial tension can be obtained as

$$\mathbf{K}_t(\omega) = \begin{bmatrix} K_{t11} & K_{t12} & K_{t13} & K_{t14} \\ K_{t21} & K_{t22} & K_{t23} & K_{t24} \\ K_{t31} & K_{t32} & K_{t33} & K_{t34} \\ K_{t41} & K_{t42} & K_{t43} & K_{t44} \end{bmatrix} \quad (38)$$

Because the detailed expression of K_{ij} is very complex, it is not presented here. The expression can be obtained directly via symbolic computation using mathematical software based on Eq. (34).

3.4 Element stiffness matrix

Assembling the axial stiffness matrix, the bending stiffness matrix and the stiffness matrix of the initial axial force given in Eqs. (19), (29) and (38), the total stiffness matrix of the element is obtained as follows

$$\mathbf{K}_e(\omega) = \begin{bmatrix} K_{u11} & 0 & 0 & K_{u14} & 0 & 0 \\ 0 & K_{v11} + K_{t11} & K_{v12} + K_{t11} & 0 & K_{v13} + K_{t11} & K_{v14} + K_{t11} \\ 0 & K_{v21} + K_{t21} & K_{v22} + K_{t22} & 0 & K_{v23} + K_{t23} & K_{v24} + K_{t24} \\ K_{u41} & 0 & 0 & K_{u44} & 0 & 0 \\ 0 & K_{v31} + K_{t31} & K_{v32} + K_{t32} & 0 & K_{v33} + K_{t33} & K_{v34} + K_{t34} \\ 0 & K_{v41} + K_{t41} & K_{v42} + K_{t42} & 0 & K_{v43} + K_{t43} & K_{v44} + K_{t44} \end{bmatrix} \quad (39)$$

3.5 Element mass matrix

The potential energy due to the axial inertia force is

$$\Pi_{f1} = \int_0^l -m(\ddot{u})u dx \quad (40)$$

The variation of the potential energy is

$$\begin{aligned} \delta \Pi_{f1} &= \int_0^l -m(\ddot{u})\delta u dx \\ &= -m \int_0^l \delta \mathbf{u}^T \mathbf{N}_u^T \mathbf{N}_u \ddot{\mathbf{u}} dx \\ &= -\delta \mathbf{u}^T m \int_0^l \mathbf{N}_u^T \mathbf{N}_u dx \ddot{\mathbf{u}} \end{aligned} \quad (41)$$

The consistent mass matrix of the element is obtained as

$$\mathbf{M}_1(\omega) = m \int_0^l \mathbf{N}_u^T \mathbf{N}_u dx = \begin{bmatrix} M_{11} & M_{14} \\ M_{41} & M_{44} \end{bmatrix} \quad (42)$$

where

$$\begin{aligned} M_{11} = M_{44} &= \frac{m(\alpha l - \sin(\alpha l)\cos(\alpha l))}{2\alpha \sin^2(\alpha l)} \\ M_{14} = M_{41} &= \frac{m(\sin(\alpha l) - \alpha l \cos(\alpha l))}{2\alpha \sin^2(\alpha l)} \end{aligned} \quad (43)$$

The potential energy due to the transverse inertia force is

$$\Pi_{f2} = \int_0^l -m(\ddot{v})v dx \quad (44)$$

The variation of the potential energy is

$$\begin{aligned} \delta \Pi_{f2} &= \int_0^l -m(\ddot{v})\delta v dx \\ &= -m \int_0^l \delta \mathbf{v}^T \mathbf{N}_v^T \mathbf{N}_v \ddot{\mathbf{v}} dx \\ &= -\delta \mathbf{v}^T m \int_0^l \mathbf{N}_v^T \mathbf{N}_v dx \ddot{\mathbf{v}} \end{aligned} \quad (45)$$

The corresponding mass matrix is obtained as

$$\begin{aligned} \mathbf{M}_2(\omega) &= m \int_0^l \mathbf{N}_v^T \mathbf{N}_v dx \\ &= \begin{bmatrix} M_{22} & M_{23} & M_{25} & M_{26} \\ & M_{33} & M_{35} & M_{36} \\ & & M_{55} & M_{56} \\ \text{symmetry} & & & M_{66} \end{bmatrix} \end{aligned} \quad (46)$$

Note that the detailed expression of M_{ij} is very complex, thus it is not presented here. The expression can be obtained directly via symbolic computation using mathematical software based on Eq. (45).

Assembling the potential energy due to the axial inertia force and the transverse inertia force given in Eqs. (42) and (46), the consistent mass matrix of the element is obtained as follows

$$\mathbf{M}_e(\omega) = \begin{bmatrix} M_{11} & 0 & 0 & M_{14} & 0 & 0 \\ & M_{22} & M_{23} & 0 & M_{25} & M_{26} \\ & & M_{33} & 0 & M_{35} & M_{36} \\ & & & M_{44} & 0 & 0 \\ & & & & M_{55} & M_{56} \\ \text{symmetry} & & & & & M_{66} \end{bmatrix} \quad (47)$$

4. Algorithm and programming

Once the stiffness and mass matrices of the element are obtained, the global stiffness and mass matrices of the beam can be obtained by using the general assembly method of the conventional finite element method. The equations of motion for an un-damped free vibration system can be expressed as the following form

$$\mathbf{K}(\omega)\mathbf{D} + \mathbf{M}(\omega)\ddot{\mathbf{D}} = \mathbf{0} \quad (48)$$

where $\mathbf{K}(\omega)$ and $\mathbf{M}(\omega)$ are the global stiffness and mass

matrices, respectively, $\mathbf{0}$ is a zero vector, and \mathbf{D} is the vector of nodal displacement, $\dot{\mathbf{D}}$ is the second time derivative of nodal displacement.

For an un-damped structure, the general solution of the nodal displacement can be expressed as

$$D(t, x) = \phi(x) \sin(\omega t + \theta) \quad (49)$$

Substituting Eq. (49) into (48) gives

$$[\mathbf{K}(\omega) - \omega^2 \mathbf{M}(\omega)] \mathbf{D} = 0 \quad (50)$$

By definition, \mathbf{D} in Eq. (50) must have a nontrivial solution, thus,

$$\|\mathbf{K}(\omega) - \omega^2 \mathbf{M}(\omega)\| = 0 \quad (51)$$

Eq. (51) is called the frequency equation of the system. By solving this equation, the natural frequencies and frequency vectors can be obtained.

The proposed method is called the dynamic finite element method because both the stiffness matrix $\mathbf{K}(\omega)$ and the mass matrix $\mathbf{M}(\omega)$ are dynamic and the values are related to the frequencies.

Different from the static finite element method, the stiffness and mass matrices of the new element are exact for a specified frequency; as a result, the shape functions of different natural frequencies are different. Frequency Eq. (51) must be solved by using the iterative method. There are two types of engineering problems: one is the natural frequency calculation of a beam with a given axial force, and the other is the axial force estimation of a beam with a measured frequency.

4.1 Natural frequency calculation for a given axial force

Fig. 2 shows the iterative algorithm for the natural frequencies calculation of a beam with a given axial force by using the proposed new dynamic element. During the iteration procedure the shape function of the element is updated. The iteration details are as follows:

1. Set the initial frequency vector as $\omega(0) = \{\omega_1(0) \ \omega_2(0) \ \dots \ \omega_n(0)\} = \mathbf{0}$, in which $\mathbf{0}$ is a zero vector. The first iteration is started as $\omega = \omega_1(0) = 0$.

Substituting $\omega = \omega_1(0) = 0$ into Eq. (1) yields $\alpha = \varepsilon = \delta = 0$; thus, the proposed new element is degenerated as the conventional beam element considering the effect of the axial force. By solving Eq. (51), the first set of approximate frequencies $\omega(1) = \{\omega_1(1) \ \omega_2(1) \ \dots \ \omega_n(1)\}$ is obtained.

2. Set the value of current frequency to the value calculated from the first iteration, $\omega = \omega_1(1)$. New global stiffness matrix $\mathbf{K}(\omega)$ and mass matrix $\mathbf{M}(\omega)$ are reformed. Solving the corresponding eigenvalue problem yields the second set of approximate frequencies $\omega(2) = \{\omega_1(2) \ \omega_2(2) \ \dots \ \omega_n(2)\}$.

3. If $|\omega_1(1) - \omega_1(2)| \leq Tol$, where Tol is the predefined

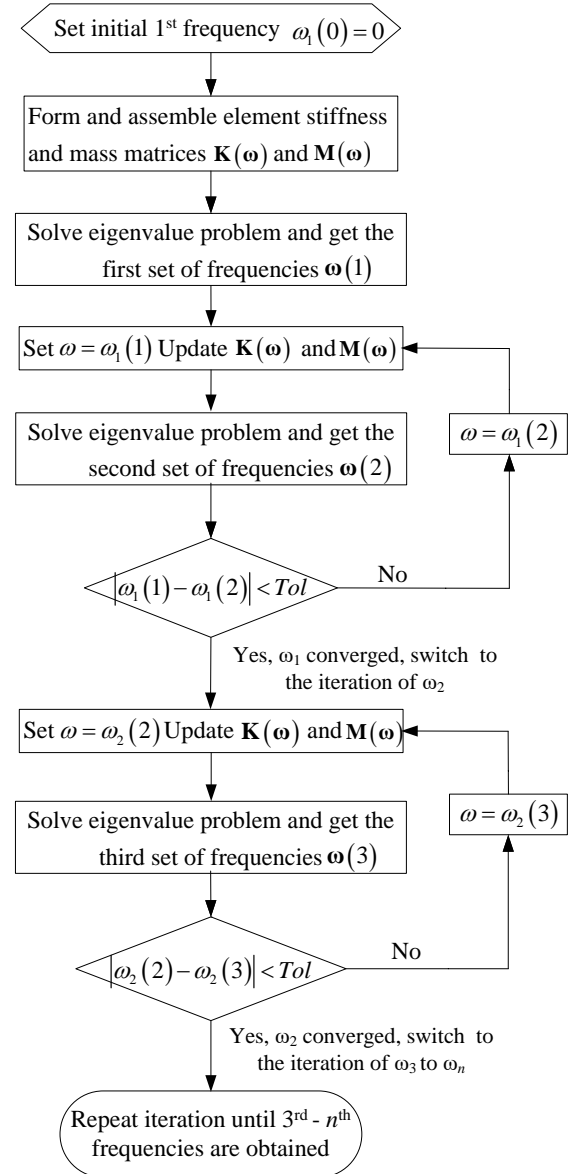


Fig. 2 Algorithm for the exact natural frequencies calculation

convergence tolerance, then the iteration is terminated and the final value of the first order frequency is $\omega_1 = \omega_1(2)$; go to step 4 to calculate the second order frequency. If the convergence condition is not satisfied, then repeat step 2 until the difference between the frequency results of the two adjacent iterations satisfies the convergence tolerance.

4. Set $\omega_2 = \omega_2(2)$ to obtain the iterative solution of the second order frequency. New global stiffness matrix $\mathbf{K}(\omega)$ and mass matrix $\mathbf{M}(\omega)$ are reformed. Solving the eigenvalue Eq. (51) yields the third set of approximate frequencies $\omega(3) = \{\omega_1(3) \ \omega_2(3) \ \dots \ \omega_n(3)\}$.

5. If $|\omega_2(2) - \omega_2(3)| \leq Tol$, where Tol is the predefined convergence tolerance, then the iteration is terminated and the final value of the second order frequency is $\omega_2 = \omega_2(3)$; go to the next step to calculate the next order frequency. If

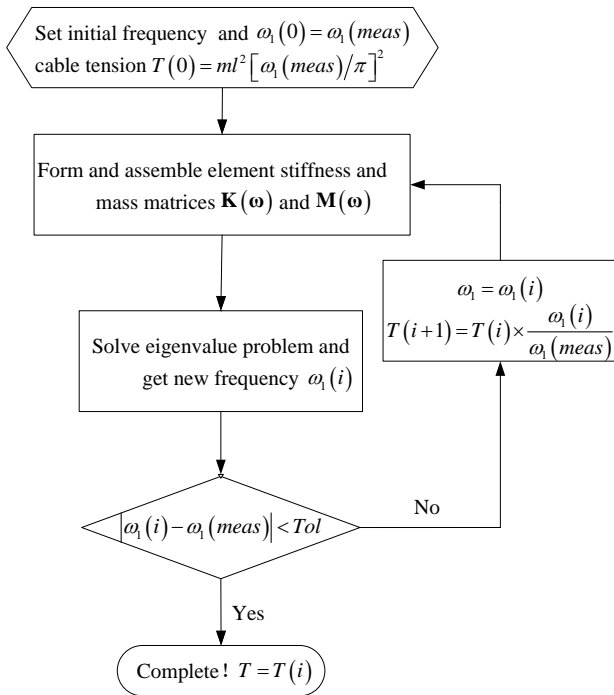


Fig. 3 Algorithm for cable tension estimation using the exact dynamic element

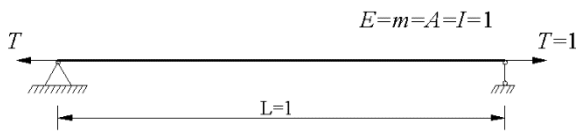


Fig. 4 Simple supported beam

the convergence condition is not satisfied, then repeat step 4 until the difference between frequency results of two adjacent iterations satisfies the convergence tolerance.

6. Set $\omega_n = \omega_n(n)$ to obtain the iterative solution until all of the frequencies required are calculated. Based on the above steps, a program for the natural frequency calculation of a beam with a given axial force was established using MATLAB as shown in Fig.2.

4.2 Axial force estimation from a measured frequency

Another engineering problem is determining the axial force when the frequencies of the beam are measured. This problem is valuable in the cable tension estimation of cable-supported structures. As in the cable tension estimation, an iterative method is required because two parameters ω and T must be updated. The iteration details of the use of the measured first order frequency to estimate the axial force are illustrated as follows:

1. In the first iteration, set $\omega_1(0) = \omega_1(meas)$ and $T(0) = ml^2 [\omega_1(meas)/\pi]^2$, where $\omega_1(meas)$ is the measured first order circular frequency, and m and l are the mass per unit length and the length of the beam, respectively. The stiffness and mass matrices of the new

beam element can be obtained by substituting the values of ω and T into Eqs. (39) and (47). Next, the global stiffness matrix $\mathbf{K}(\omega)$ and the mass matrix $\mathbf{M}(\omega)$ can be obtained according to the order of the degrees of freedom. By solving Eq. (51), the first set of approximate solutions $\omega_1(1)$ and $T(1)$ are obtained.

2. If $|\omega_1(1) - \omega_1(meas)| \leq Tol$, where Tol is the predefined convergence tolerance, then the iteration is terminated, and the final value of the axial force is $T = T(1)$. If the convergence condition is not satisfied, set $\omega = \omega_1(1)$ and $T = T(1) \times \omega_1(1) / \omega_1(meas)$, return to step 1 to update the global stiffness and mass matrices and obtain another set of approximate solutions $\omega(i)$ and $T(i)$, and then repeat the iteration until the difference between frequency results of two adjacent iterations satisfies the convergence tolerance.

Based on the above steps, a program for the axial force estimation of a beam with a measured frequency was established using MATLAB. The algorithm for cable tension estimation using the exact dynamic element is shown in Fig. 3.

5. Examples

5.1 Natural frequency analysis of a simple supported beam

Fig. 4 shows a simple supported beam with the parameters $E=m=A=I=T=L=1$. The natural frequencies of the transverse vibration of the beam can be calculated using the following equation (Clough and Penzien 1995)

$$\omega_n = \frac{n^2 \pi^2}{L^2} \sqrt{1 + \frac{TL^2}{n^2 \pi^2 EI}} \sqrt{\frac{EI}{m}} \quad (52)$$

The first eight frequencies of the beam calculated using Eq. (52) are listed in Table 1.

The beam is modeled with four meshes using the new dynamic element and the algorithm proposed in this paper. The result of frequency iteration, starting with initial frequency $\omega_0=0$, is shown in Table 2. From the iteration history, the first, second and third natural frequencies converge to the exact solutions in three, seven and twelve iterations, respectively.

Using the proposed new element and algorithm, the calculated results with 4 new elements are exactly the same as the analytical solutions with six digits after the decimal point. But, when using the conventional beam element which is a static element based on Bernoulli-Euler theory, much more elements are required to obtain a similar accuracy solution. Solutions of frequency with different meshes using the conventional beam elements are summarized in Table 3. For the third order frequency, the results calculated from the mesh consisting of 256 conventional beam elements are found to be the same as those obtained by using 4 dynamic beam elements within twelve iterations. That is to say, in order to obtain results

Table 1 Exact frequencies of the simple supported beam

| n | 1 | 2 | 3 | 4 | 5 | 6 | 7 | 8 |
|------------|----------|----------|-----------|-----------|-----------|-----------|-----------|------------|
| ω_n | 1.648454 | 6.362265 | 14.216522 | 25.212193 | 39.349405 | 56.628189 | 77.048556 | 100.610511 |

Table 2 Solution history of frequencies with four dynamic beam elements

| Iteration | ω_0 | ω_1 | ω_2 | ω_3 | Difference (%) | Notes |
|-----------|------------|------------|------------|------------|----------------|-------------------------|
| 1 | 0.000000 | 1.648843 | 6.386787 | 14.473669 | - | |
| 2 | 1.648843 | 1.648454 | 6.383678 | 14.463397 | 2.361E-02 | |
| 3 | 1.648454 | 1.648454 | 6.381683 | 14.462765 | 0.000E+00 | ω_1 converged |
| 4 | 6.381683 | | 6.370486 | 14.456250 | 3.052E-01 | |
| 5 | 6.370486 | | 6.362694 | 14.436259 | 1.292E-01 | |
| 6 | 6.362694 | | 6.362265 | 14.416265 | 6.745E-03 | |
| 7 | 6.362265 | | 6.362265 | 14.404511 | 0.000E+00 | ω_2 converged |
| 8 | 14.404511 | | | 14.265824 | 1.322E+00 | |
| 9 | 14.265824 | | | 14.220717 | 3.468E-01 | |
| 10 | 14.220717 | | | 14.216552 | 2.951E-02 | |
| 11 | 14.216552 | | | 14.216522 | 2.118E-04 | |
| 12 | 14.216522 | | | 14.216522 | 0.000E+00 | ω_3 converged |

Table 3 Solutions of frequency with different meshes using the conventional beam element

| Number of elements | ω_1 | ω_2 | ω_3 |
|--------------------|------------|------------|------------|
| 4 | 1.648843 | 6.386787 | 14.473669 |
| 8 | 1.648479 | 6.363877 | 14.234615 |
| 16 | 1.648456 | 6.362367 | 14.217685 |
| 32 | 1.648454 | 6.362271 | 14.216595 |
| 64 | 1.648454 | 6.362265 | 14.216526 |
| 128 | 1.648454 | 6.362265 | 14.216523 |
| 256 | 1.648454 | 6.362265 | 14.216522 |
| Exact solutions | 1.648454 | 6.362265 | 14.216522 |

of similar accuracy for the first three modes, eigenvalue problems with 15 DOFs are solved twelve times by using the new dynamic element, while eigenvalue problems with 771 DOFs are solved by using the conventional beam element. The total number of linear equations should be solved are 180 and 771 for models with new dynamic element and conventional beam element, respectively. So, the computational time should be greatly reduced using the dynamic element. Moreover, for higher order frequencies or for large models, the savings in computational time using the new element can be more significant.

Comparisons of the solution times using the proposed dynamic element and the conventional beam element are shown in Table 4. All of the models are calculated using an Acer M3970 PC with a four-core Intel i5-2300 2.8 GHz CPU and AMD Radeon HD 6570 graphics card. From the table, the computational time is reduced significantly using

Table 4 Comparison of the solution times and the mesh divisions

| | | ω_1 | ω_2 | ω_3 |
|--------------------------|-----------------------|------------|------------|------------|
| Conventional element | Computational time(s) | 0.051 | 0.152 | 2.161 |
| | Mesh divisions | 32 | 64 | 256 |
| Proposed dynamic element | Computational time(s) | 0.042 | 0.127 | 0.913 |
| | Mesh divisions | 2 | 3 | 4 |

Table 5 Comparison of the estimated cable tension

| | Proposed element (4 elements) | Conventional element (4 elements) | Conventional element (128 elements) |
|----------------------|-------------------------------|-----------------------------------|-------------------------------------|
| Estimation results | 1.0000 | 0.9814 | 0.9997 |
| Difference (%) | 0.00% | 1.86% | 0.03% |
| Calculation time (s) | 0.56 | 0.33 | 3.75 |

the proposed method, especially for large models and high order frequencies.

5.2 Cable tension estimation

For the same example shown in Fig. 4, according to Eq. (52), the exact internal force can be expressed using the measured frequency as

$$T = \frac{m\omega_n^2 l^2}{n^2 \pi^2} - \frac{n^2 \pi^2}{l^2} EI \tag{53}$$

Assuming that the measured frequencies have the values of the theoretical results, the axial force of the cable can be estimated accurately using the method described in section 4.2. The beam is meshed with 4 proposed elements or 64 conventional beam elements, and the measured frequency is the first order calculated natural frequency i.e. $\omega_1=1.648454$. The cable tension estimation results and computational times are listed in Table 5. From the table, no difference is found between the real cable force and the calculated one using the proposed dynamic finite element method. While the difference between the real cable force and the calculated one using the conventional beam element are 1.86% and 0.03% when the beam is meshed with 4 elements and 128 elements, respectively.

So, the proposed method is more efficient. To obtain the same accuracy, the conventional beam element method requires more computational time: nearly 6.7 times that of the proposed method.

6. Conclusions

Based on the general solutions of the homogeneous dynamic equilibrium equation for un-damped vibration of an axially loaded beam, new element shape functions were derived and a novel dynamic beam element was developed for the exact natural frequency calculation and cable tension estimation of a cable considering bending stiffness.

Combining the new dynamic element and conventional finite element method, iteration algorithms were proposed for exact natural frequency calculation and cable tension estimation. The program of cable tension identification based on the proposed dynamic beam element was also developed using MATLAB. The illustrative examples showed that the method proposed in this paper has a distinct advantage on the accuracy and computational time compared with a conventional beam element, both in natural frequency calculation and in axial force estimation. In addition, the savings in computational time achieved with the new element can be quite significant, especially for large models. This new method can be widely applied to determine the cable tension in cable supported structures accurately and efficiently, especially for real-time structural monitoring, which requires fast calculation.

Acknowledgments

The authors gratefully acknowledge the financial supports from the National Natural Science Foundation of China (Grant No. 51678169), the Technology Planning Project of Guangdong Province (Grant No. 2016B050501004), the Pearl River S&T Nova Program of Guangzhou (Grant No. 201710010147) and the Research Project of Guangzhou Municipal Education Bureau (Grant No. 1201620446).

References

- Banerjee J.R. (1989), "Coupled bending-torsional dynamic stiffness matrix for beam elements", *Int. J. Numer. Meth. Eng.*, **28**(6), 1283-1289.
- Banerjee J.R. (1997), "Dynamic stiffness formulation for structural elements: a general approach", *Comput. Struct.*, **63**(1), 101-103.
- Banerjee, J.R. and Fisher, S.A. (1992), "Coupled bending-torsional dynamic stiffness matrix for axially loaded beam elements", *Int. J. Numer. Meth. Eng.*, **33**(4), 739-751.
- Banerjee, J.R. and Williams, F.W. (1985), "Exact Bernoulli-Euler dynamic stiffness matrix for a range of tapered beams", *Int. J. Numer. Meth. Eng.*, **21**(12), 2289-2302.
- Banerjee, J.R. and Williams, F.W. (1992), "Coupled bending-torsional dynamic stiffness matrix for Timoshenko beam elements", *Comput. Struct.*, **42**(3), 301-310.
- Bao, Y.Q., Shi, Z.Q., Beck, J.L., Li, H. and Hou, T.Y. (2017), "Identification of time-varying cable tension forces based on adaptive sparse time-frequency analysis of cable vibrations", *Struct. Contr. Health Monitor.*, **24**(3).
- Cheng, F.Y. (1970), "Vibration of Timoshenko beams and frameworks", *J. Struct. Div.*, **96**(3), 551-571.
- Cheng, F.Y. and Tseng, W.H. (1973), "Dynamic matrix of Timoshenko beam columns", *J. Struct. Div.*, **99**(3), 527-549.
- Clough, R.W. and Penzien, J. (1995), *Dynamics of Structures*, 3rd Edition, Computer & Structures, Inc., Berkeley, U.S.A.
- Friberg, P.O. (1983), "Coupled vibration of beams-an exact dynamic element stiffness matrix", *Int. J. Numer. Meth. Eng.*, **19**(4), 479-493.
- Hallauer, W.L. and Liu, R.Y.L. (1982), "Beam bending-torsion dynamic stiffness method for calculation of exact vibration modes", *J. Sound Vibr.*, **85**(1), 105-113.
- Hashemi, S.M. and Richard, M.J. (2000), "A dynamic finite element (DFE) method for free vibrations of bending-torsion coupled beam", *Aerosp. Sci. Technol.*, **4**(1), 41-55.
- Howson, W.P. and Williams, F.W. (1973), "Natural frequencies of frames with axially loaded Timoshenko members", *J. Sound Vibr.*, **26**(4), 503-515.
- Huang, Y.H., Fu, J.Y., Gan, Q., Wang, R.H., Pi, Y.L. and Liu, A.R. (2017), "New method for identifying internal forces of hangers based on form-finding theory of suspension cable", *J. Brid. Eng.*, **22**(11), 96-105.
- Huang, Y.H., Fu, J.Y., Wang, R.H., Gan, Q. and Liu, A.R. (2015), "Unified practical formulas for vibration-based method of cable tension estimation", *Adv. Struct. Eng.*, **18**(3), 405-422.
- Huang, Y.H., Fu, J.Y., Wang, R.H., Gan, Q., Rao, R. and Liu, A.R. (2015), "Practical formula to calculate tension of vertical cable with hinged-fixed conditions based on vibration method", *J. Vibroeng.*, **16**(2), 997-1009.
- Issa, M.S. (1988), "Natural frequencies of continuous curved beams on Winkler-type foundation", *J. Sound Vibr.*, **127**(2), 291-301.
- Kalousek, V. (1973), *Dynamics in Engineering Structures*, Butterworths, London, U.K.
- Kim, B.H. and Park, T. (2007), "Estimation of cable tension force using the frequency-based system identification method", *J. Sound Vibr.*, **304**(3-5), 660-676.
- Kim, J.M., Lee, J. and Sohn, H. (2018), "Detection of tension force reduction in a post-tensioning tendon using pulsed-eddy-current measurement", *Struct. Eng. Mech.*, **62**(2), 129-139.
- Kolousek, V. (1941), "Anwendung des Gesetzes der virtuellen Verschiebungen und des Reziprozitätssatzes in der Stabwerksdynamic", *Arch. Appl. Mech.*, **12**(6), 363-370.
- Leung, A.Y.T. (1992), "Dynamic stiffness for lateral buckling", *Comput. Struct.*, **42**(3), 321-325.
- Liao, W.Y., Ni, Y.Q. and Zheng, G. (2012), "Tension force and structural parameter identification of bridge cables", *Adv. Struct. Eng.*, **15**(6), 983-995.
- Lunden, R. and Akesson, B.A. (1983), "Damped second-order Rayleigh-Timoshenko beam vibration in spacean exact complex dynamic member stiffness matrix", *Int. J. Numer. Meth. Eng.*, **19**(3), 431-449.
- Ma, H.T. (2008), "Exact solutions of axial vibration problems of elastic bars", *Int. J. Numer. Meth. Eng.*, **16**(5), 241-252.
- Ma, H.T. (2010), "Exact solution of vibration problems of frame structures", *Commun. Numer. Meth. Eng.*, **26**(5), 587-596.
- Ma, L. (2017), "A highly precise frequency-based method for estimating the tension of an inclined cable with unknown boundary conditions", *J. Sound Vibr.*, **409**, 65-80.
- Maes, K., Peeters, J., Reynders, E., Lombaert, G. and Roeck, G.D. (2017), "Identification of axial forces in beam members by local vibration measurements", *J. Sound Vibr.*, **332**(21), 5417-5432.
- Mohammadnejad, M. and Kazemi, H.H. (2018), "A new and simple analytical approach to determining the natural frequencies of framed tube structures", *Struct. Eng. Mech.*, **56**(6), 939-957.
- Mohsin, M.E. and Sadek, E.A. (1968), "The distributed mass-stiffness technique for the dynamical analysis of complex frameworks", *Struct. Eng.*, **46**(11), 345-351.
- Park, D.U. and Kim, N.S. (2014), "Back analysis technique for tensile force on hanger cables of a suspension bridge", *J. Vibr. Contr.*, **20**(5), 761-772.
- Wang, J., Liu, W.Q., Lu, W. and Han, X.J. (2015), "Estimation of main cable tension force of suspension bridges based on ambient vibration frequency measurements", *Struct. Eng. Mech.*, **56**(6), 939-957.
- Wang, R.H., Gan, Q., Huang, Y.H. and Ma, H.T. (2011), "Estimation of tension in cables with intermediate elastic supports using finite-element method", *J. Brid. Eng.*, **16**(5), 675-678.

- Wang, T.M. and Kinsman, T.A. (1970), "Vibration of frame structures according to the Timoshenko theory", *J. Sound Vibr.*, **14**(2), 215-227.
- Williams, F.W. and Kennedy, D. (1987), "Exact dynamic member stiffnesses for a beam on an elastic foundation", *Earthq. Eng. Struct. Dyn.*, **15**(1), 133-136.
- Wittrick, W.H. and Williams, F.W. (1971), "A general algorithm for computing natural frequencies of elastic structures", *Quarter. J. Mech. Appl. Math.*, **24**(3), 263-284.
- Yan, B.F., Yu, J.Y. and Soliman, M. (2015), "Estimation of cable tension force independent of complex boundary conditions", *J. Eng. Mech.*, **141**(1), 15-22.
- Yuan, S., Ye, K.S., Xiao, C., Williams, F.W. and Kennedy, D. (2007), "Exact dynamic stiffness method for non-uniform Timoshenko beam vibrations and Bernoulli-Euler column buckling", *J. Sound Vibr.*, **303**(1), 526-537.
- Yucel, A., Arpacı, A. and Tufekci, E. (2014), "Coupled axial-flexural-torsional vibration of Timoshenko frames", *J. Sound Vibr.*, **20**(15), 2366-2377.
- Zarhaf, S.E.H.A.M., Norouzi, M., Allemang, R.L., Hunt, V.J., Helmicki, A. and Nims, D.K. (2017), "Stay force estimation in cable-stayed bridges using stochastic subspace identification methods", *J. Brid. Eng.*, **22**(9), 04017055.
- Zienkiewicz, O.C. and Taylor, R.L. (2000), *The Finite Element Method for Solid and Structural Mechanics*, 2nd Edition, Butterworth-Heinemann, Oxford.